Molecular Systems Design & Engineering 2021,**6**, 997-1002

DOI: https://doi.org/10.1039/D1ME00066G

Microstructure study of fractured polar bear hair for toughening, strengthening, stiffening designs via energy dissipation and crack deflection mechanisms in materials

Urszula Stachewicz[1]*

[1] Faculty of Metals Engineering and Industrial Computer Science, AGH University of Science and Technology, Al. A. Mickiewicza 30, 30-059 Kraków, Poland

*Corresponding author email address: ustachew@agh.edu.pl

Keywords: polar bear, hair, keratin, SEM, crack propagation, microstructure

Abstract

Polar bear hair is known for its superior thermal insulation properties protecting from frigid water and freezing weather conditions. However, this microscopy study of polar bear hair is related to the investigation of the crack stopping mechanisms within its structure following the toughening mechanism principle used by nature. The inhomogeneous structure of polar bear hair consists of fiber bundles, tubules, membranes, porous medulla, and cuticle layers. Precisely, these types of material constructions help in impact energy dissipation to protect material before the failure and save animals via its multifunctionality. The multiscale structures are the key to adopting different physical properties in distinct sizes, from thermal insulation to the toughening, strengthening, and stiffening mechanisms in material designs.

Introduction

Understanding the structure-function relationship is key in developing new materials. Natural materials are one of the best inspirations, as we could see throughout many available technologies.[1, 2] The building blocks of many natural materials are proteins such as collagen, keratin, and silk.[3-9] Inspirational examples are found in bone,[10] nacre,[11] crocodile skin,[12] peacock feather, [13] and many more.[14] The other key feature is the hierarchical structure primarily related to enhancing the mechanical properties.[3, 14, 15] The geometry, together with the distinct components, plays an important role in fracture resistance of natural materials or tissues. [16-19] The damage process involves cracks promotion and propagation, considered an intrinsic toughening mechanism. The formation of cracks, especially in the brittle ceramic materials, starts with a tip that is usually the damaging mechanism that can be transformed to intrinsic toughening when the material's microstructure allows. Otherwise, extrinsically it involves the crack bringing which is the example of the shielding mechanism in the crack propagation. [20] In case of polymeric materials the ductile behaviors' cause the plastic deformation [21] also in the natural polymers and biomass.[22]

Keratin is an example of a natural polymer with a low extension, especially at low humidity (< 30 %) it is below 40 % . [23] This structural protein is present, for instance, in the turtle carapace, layered with collagen. This keratin collagen bi-layer enhanced resistance to crack growth, increased toughness, and increase plastic dissipation of carapace at their interfaces, allowing increase energy dissipation to ensure the protection of the turtles. [24] In compact bone, collagen is combined with hydroxyapatite (HA) to alternate high and low stiffness in osteons. This mechanical design with the variable collagen fiber orientation and mineral content uses composition strategies at the sublamellar level to prevent microcracks leading to bone failure.[18] The feather represents a mechanically rebuts and flexible keratin-based material with HA. The hierarchical structure of feathers with fibrous cortex and foamy medulla is using HA crystals as stiffeners. The mechanical strength under tension or compression is achieved due to delamination, intralamellar debonding, fibers splitting and bridging, and fibers rapture. The cracks are bridged by fibers bundles

oriented at different angles, similar to in the compact bone by lamellae, to hinder its propagation. This mechanism contributes to the higher resistance to fracture in feathers.[13]

Most natural and nature-inspired materials have extrinsic toughening mechanisms. In the examples mentioned above, fracture resistance increases with a crack extension due to the shielding mechanism involved in its propagation. Notably, rigid and robust materials design requires tailoring structural properties, synergetic strengthening, and stiffening effects at the optimum combination. The multiscale structures, including porosity and fibers created by nature, are particularly good at reinforcements and hindering fractures, leading to preferred mechanical properties. The flaw tolerance, not only in natural materials, is easier to manage in porous materials or composite with nanofibers, enhancing stress dissipation in the constructions.[13] Particularly, the delocalization of stress in the electrospun fiber meshes was investigated in notched samples during the tensile testing. The visual observation of strain distribution allowed the material deformation analysis. Notably, the network of nanofibers deformed relatively homogeneously throughout the membrane without the stress concentration at the incorporated cracks. In opposition to fibers, the polymer films were exposed to intense stress concentration at the notches.[25] Importantly, microcracks are tolerated in the randomly oriented electrospun meshes and the spider webs, avoiding catastrophic failures. [26] Therefore, polymer nanofibers are widely used as a reinforcement in the composites in the form of the whole network of fibers or short fibers, [27] where the proper integration between nanofibers and matrix is crucial for the optimized mechanical performance of produced composites.[28] One of the critical elements is the high volume fraction of nanofibers. Extreme cases of the strongest materials in biology, such as limpet teeth, hold the record for biological material in having the highest tensile strength. [29] Another important element is the critical length of fibers used in the reinforcements in composites [30] and core-shell structures.[31].The fragmented fibers from brittle polymers can be used as a short fibers as the reinforcements in of composites. In composites optimization the incorporation of the nanofillers increases the materials' stiffness however it may also cause the brittle fracture. [32]

Similarly to polymer fibers,[33] hair fur is most exposed to environmental conditions, affecting their mechanical properties.[34] Concerning the extreme weather conditions, the polar bear hair provides excellent thermal and water insulation and protection.[35-38] Hair has various functions according to species.[39] To understand strategies created by nature to obtain insulating, hydrophobic, and mechanically robust materials the profound analyses of their microstructure are necessary. Previously, we investigated in detail polar bears' hair structure compared to the penguin feather, looking for the key features for designing fiber structures with high insulation properties.[40] High-resolution scanning electron microscopy (SEM) was used to observe the optimized microstructure of feather and polar bear and compare them to find common characteristics necessary for highly insulating keratin-based materials. Both materials are hierarchically porous and are formed with keratin nanofibers forming bundles and with the additional tubular porosity located between them. Basically, the hierarchical structures of natural materials allow accommodating many vital parameters such as flexibility and mechanical robustness. The microstructural design strategies in polar bear hair are unique due to their UV absorption properties [41] and adaptation of fur to match the varying needs of insulation in terrestrial and aquatic modes of life.[42] The microstructure of polar bear hair is ingenious from the fracture-mechanics perspective due to resistance to dry, wet, and freezing environmental conditions—the development of new materials for structural applications demands combinations of strength and toughness. Therefore, the microscopy analysis of a freeze-fractured cross-section of polar bear hair was performed to visualize the presence of the crack within its structure. The nucleation and propagation of cracks primarily govern materials' fragility. The analysis of microcrack protrusion and direction through the polar bear hair structure can contribute to making materials dissipating the impact energy and lowering energy available for nucleation and propagation of cracks.

Materials and methods

The samples of polar bear (*Ursus maritimus*) hair samples were obtained from Warsaw Zoo in Poland during the medical check-up. They were also collected from the ground in the Zoo am Meer in Germany, Polar Bear Habitat of Cochrane in Canada, and Wildlife

Park, Kincraig in Scotland, UK. The imaging of the freeze-fractured cross-sections of hair was performed using scanning electron microscopy (SEM, Merlin Gemini II, Zeiss, Germany). The hair fracture was performed by bending the fibers immediately after immersing them in liquid nitrogen for a couple of minutes. All the samples were coated with a 3 nm Au layer using a rotary-pump sputter coater (Q150RS, Quorum Technologies, UK) after fixing the hair to carbon tape mounted on the SEM stubs. SEM observations were carried out with an accelerating voltage of 3-5 kV, current of 150 pA c, keeping the working distance of 3–6 mm.

Results and discussion

Polar bear hair microstructure

Polar bears have the characteristic two types of hair ground and guard built of coiled-coil α-helix keratin.[43] The cuticle is the outermost layer observed in many kinds of hair, wool, or fur. The keratin fibers are bundled along the main shaft of the hair, which is usually porous. The cortex is structured with tightly packed bundles of keratin fibers, with an average 140-180 nm diameter. In the center of the hair, the air-filled channel with a diameter of 20-30 µm, called the medulla, is located. The hollow core is typical for polar bear hair, and it was also noticed in hair from rabbits, elk, and others, but not in all species.[23] Figure 1 shows the freeze-fractured cross-section surfaces of the polar bear hair and the visible outer protective surface of the cuticle built from the flattened horny cells. Additionally, in Figures 1b-c) and 2b), the inside with the medulla is visible. Between the medulla and cuticle, there is a cortex with aligned keratin fibers reinforcing hair structure. Interestingly, the medulla is formed by the spherical hollow vacuoles, as the large pores are created in the keratinization process. The medulla consists of the lipid-rich cell membrane complex. [40]

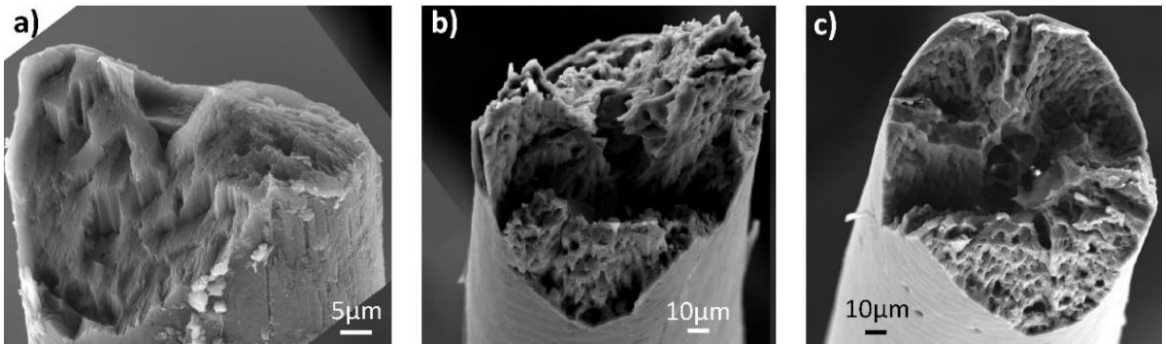

Figure 1. The cross-sections of polar bear hair showing the freeze-fractured surface, a) the fractured surface show the broken bundles of keratin b) and c) porous structure with the medulla inside the hair.

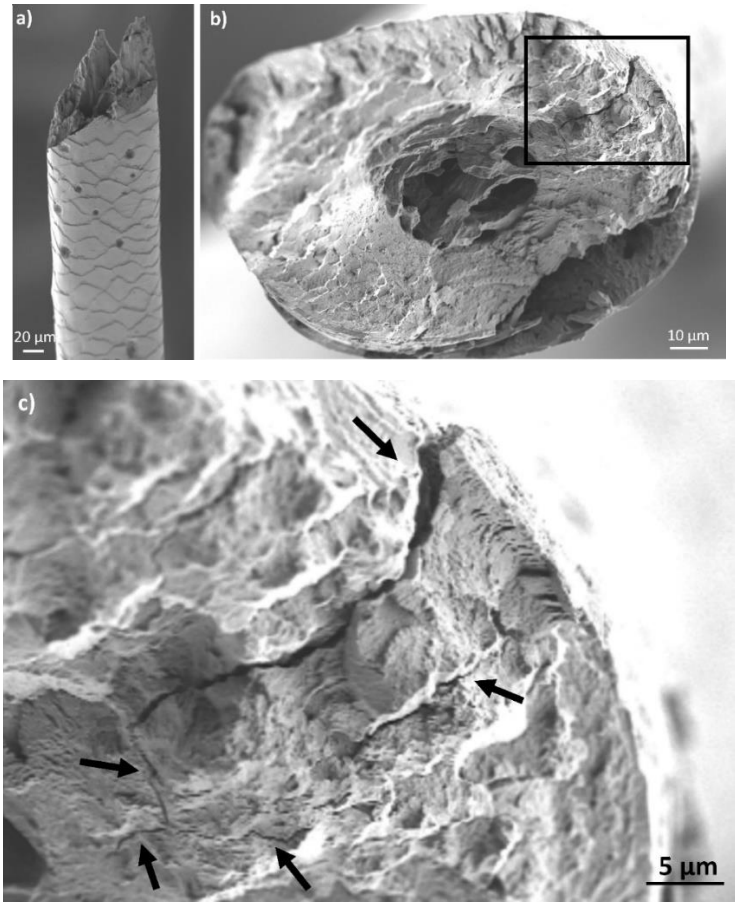

Figure 2. SEM micrographs of polar bear hair presenting a) the hair side view with the cuticle layers and overlapping scales, b) the top view, in the black square the cracks are indicated passing first the cuticle layer and then the cortex, c) the zoom from the black square magnifying cracks propagation and deflection indicated with arrows.

Tubules in crack deflection

The failure is caused by crack propagation and penetration throughout the hair structure until it is broken. After the fractionation of hair, we observed the interfacial crack deflection, see Figure 2. A few cracks are visible in Figure 2c), which begin to aggregate and interconnect during the crack propagation and finally extend, leading to material failure. The observed cracks start to propagate from the cuticular scale covering hear in a nonlinear way and stop before reaching the medulla. The medulla is the hollow part in the middle of the shaft of the hair. Notable, crack deflection is also the topographical progression that depends on the three-principal type of stress such as (i) opening, (ii) sliding, and (iii) tearing modes. From 2D SEM images, it is difficult to differentiate if the shear stress acting in parallel or perpendicular to the crack front. The gradient structure provides stress relief at the interfaces between reoriented fiber layers or bundles of keratin fibers, as shown in Figure 1a) and 3. Additionally, the tubules between the keratin bundles hinder the crack propagation, providing the hair cortex's strengthening. Interestingly, tubules are found in squid sucker ring teeth, providing excellent stability during bending for effective puncturing action actuated by their surrounding tentacle.[44] Tubules are also the microstructural features of dentin, which is the tooth's major component and middle layer, supporting the brittle enamel.[45] Dentinal tubules are peritubular channels of a few microns occupying space between mineralized and oriented collagen fibrils. Tubules are the vital features in the mechanical properties of dentine.[46, 47] Additional protection function of tubules is in compression in many bioinspired designs.[48]

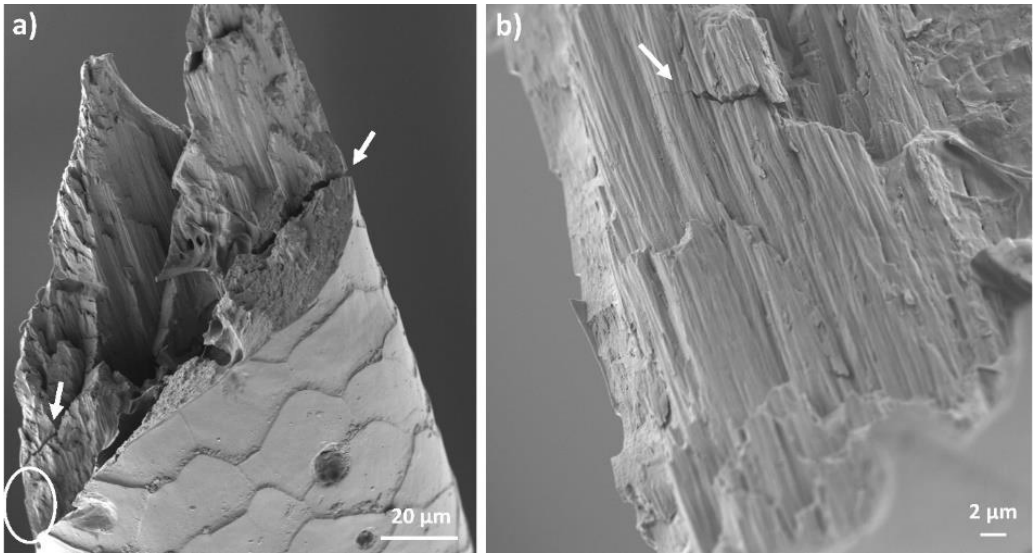

Figure 3. SEM micrographs of polar bear hair showing a) the large crack at the edge of the hair indicated with the arrows on the left and the right sides; the circled region is zoomed-in b) the crack passing throughout the bundles of keratin fibers, creating steps in the inner surface of the cortex.

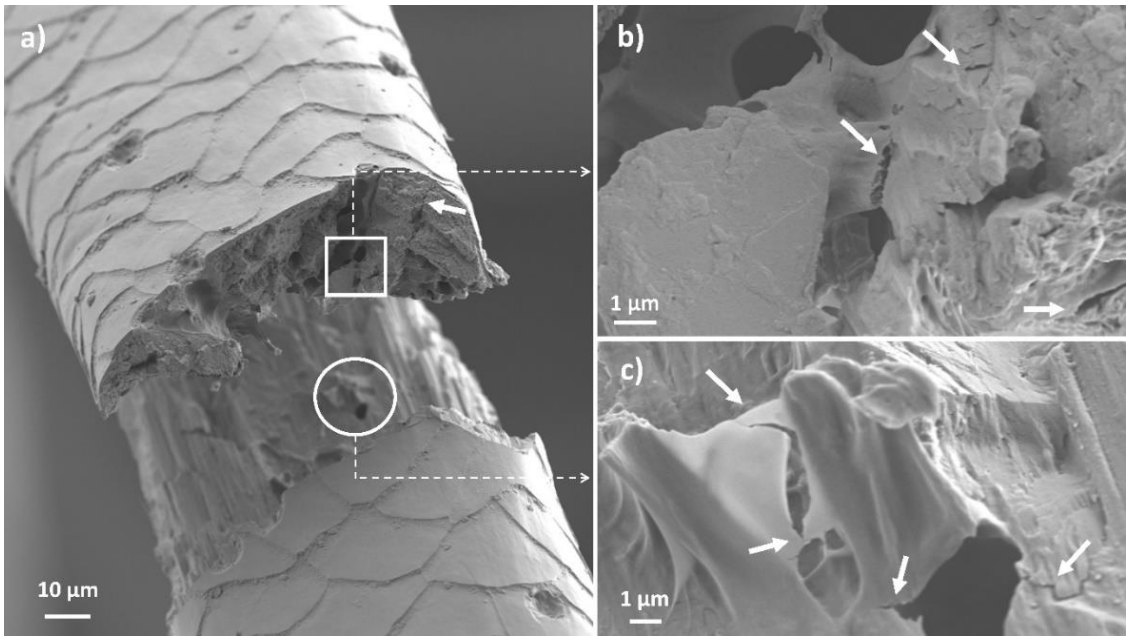

Figure 4. SEM micrographs of fractured polar bear hair presenting a) delamination showing the hollow inside, b) cracking between pores indicated with arrows, and c) cracking of medulla membrane indicated with arrows.

Energy dissipation

The high number of interfaces, such as cuticle layers and fiber bundles (see example in Figure 3), hinder crack propagation. The fractured surfaces and bridges during the introduced delamination contribute to a higher resistance to the failure. This deformation energy is absorbed before the failure of hair, which is helping in energy consumption. In Figures 2-4, the examples of cracking are indicated before the polar bear hair fracture. Usually, there are three stages in material failure: initial step, crack propagation, and failure.[49] The energy dissipation often requires parallel fibrils arrangement as it takes place in the bone.[50] The alignment of keratin fibers in the cortex (see Figure 3 b) is the intrinsic mechanism to slow down cracks progression and stops their nucleation process. Other essential mechanisms to slow crack propagation are microcracking, crack bridging, and deviation. The cracks can jump from one to the next pore leading to the imitation of the subsequent crack propagation, which happens instantaneously till the crack extension cause the failure of the material. [49] However, the crack's jump process absorbs the energy. Thus the porosity is able to block the evolution of cracks as well and is often used as a toughening effect by nature and bio-inspired structured materials.[25, 51, 52] Cellular structure resulted in much higher strength and low weight capable of resisting buckling and bending such as feather [13] or sponges.[53] In hair, the outer layer of the cuticle (see Figure 4a) is formed of scales and layers being the residual cells membrane after hair growth. It consists of intercellular lipoprotein cement providing strong cuticle cohesion. The fraction of hair has to progress through those layers to reach the internal porosity, as indicated in Figure 4b, c. The freeze-fractured hair presented in Figure 4a) shows caused delamination, followed by the cracking of the glassy membrane in Figure 4b, c. The membrane in the medulla also provides cohesion as it is considered a lipoprotein cement. Consequently, the microcracks appearing in the medulla's membrane play a significant role in toughening, as these local stress concentrations help absorb more energy. In summary, the energy dissipation, apart from the commonly used stiffing effect by adding the mineral component to the structure, is incorporated by nature by using the proteins sheets and layering, leading to an enhanced deformation process. Importantly, the natural

designs are always a compromise between strengthening, stiffening, and toughening and their combination, which is adapted to the materials' needs. The keratin fibers orientation and bundles formation, porous medulla, and cuticle layers maximize the stiffness and flexibility of polar bear hair. Similar strategies can be utilized in assembling bio-inspired synthetic materials to optimize their failure mechanics.

Conclusions

In the polar bear hair being the excellent thermal insulation design, a few toughening mechanisms were observed related to the crack sopping structures. The inhomogeneous structure consisted of fibers bundles, tubules, membranes, and layer help together with the porous medulla. The polar bear hair structure applies a few typical mechanisms for materials toughening, such as microcracking, crack bridging, branching, and delamination, helping with energy absorption. Importantly, this study showed that incorporating a tubular structure is a natural system to build the hierarchical longitudinal structures providing a path towards improving fracture resistance of man-maid fibers. This microscopy investigation indicates a crack stopping mechanism in the polar bear hair structure, which effectively protects via its porous inside. The multiscale structures are the key to adopting different physical properties in distinct sizes ranging from thermal insulation to the toughening mechanism.

Conflict of interest

There are no conflicts to declare.

Data availability statement

The data that support the study in this paper are available from the corresponding author upon reasonable request.

Acknowledgments

The author thanks Dr. Joachim Schöne, Zoo am Meer, Bremerhaven in Germany and Maria Krakowiak and dr Anna Jakucińska from Warsaw Zoo in Poland, for polar bear hair samples used in this study; Adam Gruszczyński for assistance in fracture of the hair samples and Sara Martinez -Comesana in sample preparation. This study was conducted as part of the BioCom4SavEn project funded by the European Research Council under the European Union's Horizon 2020 Framework Programme for Research and Innovation (ERC grant agreement no. 948840).

References

1. J. Aizenberg and P. Fratzl, *Adv. Funct. Mater.*, 2013, **23**, 4398-4399.
2. B. Bhushan, *Philos. T. R. Soc. A*, 2009, **367**, 1445-1486.
3. M. A. Meyers, P.-Y. Chen, A. Y.-M. Lin and Y. Seki, *Progress in Materials Science*, 2008, **53**, 1-206.
4. C.-W. Chang, J.-H. Lee and P.-h. G. Chao, *Tissue Engineering Part A*, 2019, DOI: 10.1089/ten.tea.2019.0142.
5. R. Chen and J. A. Hunt, *J. Mater. Chem.*, 2007, **17**, 3974-3979.
6. J. A. Cooper, *Proc. Natl Acad. Sci. USA*, 2007, **104**, 3049-3054.
7. G. M. Luz and J. F. Mano, *Compos. Sci. Technol.*, **70**, 1777-1788.
8. L.-D. Koh, Y. Cheng, C.-P. Teng, Y.-W. Khin, X.-J. Loh, S.-Y. Tee, M. Low, E. Ye, H.-D. Yu, Y.-W. Zhang and M.-Y. Han, *Progress in Polymer Science*, 2015, **46**, 86-110.
9. P. K. Szewczyk, J. Knapczyk-Korczak, D. P. Ura, S. Metwally, A. Gruszczynski and U. Stachewicz, *Mater. Lett.*, 2018, **233**, 211-214.
10. E. A. Zimmermann, B. Gludovatz, E. Schaible, B. Busse and R. O. Ritchie, *Biomaterials*, 2014, **35**, 5472-5481.
11. S. Gong, H. Ni, L. Jiang and Q. Cheng, *Mater. Today*, 2017, **20**, 210-219.
12. P. K. Szewczyk and U. Stachewicz, *Journal of Bionic Engineering*, 2020, **17**, 669-676.
13. Z. Q. Liu, D. Jiao, M. A. Meyers and Z. F. Zhang, *Acta Biomater*, 2015, **17**, 137-151.
14. U. G. K. Wegst, H. Bai, E. Saiz, A. P. Tomsia and R. O. Ritchie, *Nat. Mater.*, 2015, **14**, 23-36.
15. P. Fratzl and R. Weinkamer, *Progress in Materials Science*, 2007, **52**, 1263-1334.
16. P. Fratzl, H. S. Gupta, F. D. Fischer and O. Kolednik, *Adv. Mater.*, 2007, **19**, 2657-2661.
17. H. J. Gao, B. H. Ji, I. L. Jager, E. Arzt and P. Fratzl, *P. Natl. Acad. Sci. USA*, 2003, **100**, 5597-5600.
18. H. S. Gupta, U. Stachewicz, W. Wagermaier, P. Roschger, H. D. Wagner and P. Fratzl, *J. Mater. Res.*, 2006, **21**, 1913-1921.
19. S. Krauss, T. H. Metzger, P. Fratzl and M. J. Harrington, *Biomacromolecules*, 2013, **14**, 1520-1528.
20. M. E. Launey and R. O. Ritchie, *Adv. Mater.*, 2009, **21**, 2103-2110.
21. B. A. G. Schrauwen, R. P. M. Janssen, L. E. Govaert and H. E. H. Meijer, *Macromolecules*, 2004, **37**, 6069-6078.
22. D. Wilczyński, I. Malujda, K. Talaśka and R. Długi, *Procedia Engineering*, 2017, **177**, 411-418.
23. J. McKittrick, P. Y. Chen, S. G. Bodde, W. Yang, E. E. Novitskaya and M. A. Meyers, *JOM*, 2012, **64**, 449-468.

24. M. Xu and B. B. An, *Mech. Mater.*, 2020, **151**, 13.
25. U. Stachewicz, I. Peker, W. Tu and A. H. Barber, *ACS Appl. Mater. Interfaces*, 2011, **3**, 1991-1996.
26. J. M. Gosline, P. A. Guerette, C. S. Ortlepp and K. N. Savage, *J. Exp. Biol.*, 1999, **202**, 3295-3303.
27. S. Jiang, Y. Chen, G. Duan, C. Mei, A. Greiner and S. Agarwal, *Polymer Chemistry*, 2018, **9**, 2685-2720.
28. U. Stachewicz, F. Modaresifar, R. J. Bailey, T. Peijs and A. H. Barber, *ACS Appl. Mater. Interfaces*, 2012, **4**, 2577–2582.
29. A. H. Barber, D. Lu and N. M. Pugno, *J. R. Soc. Interface*, 2015, **12**, 20141326.
30. J. L. Thomason and J. L. Rudeiros-Fernández, *Frontiers in Materials*, 2018, **5**.
31. D. P. Ura, K. Berniak and U. Stachewicz, *Compos. Sci. Technol.*, 2021, **211**, 108867.
32. M. S. Enayati, R. E. Neisiany, P. Sajkiewicz, T. Behzad, P. Denis and F. Pierini, *Theoretical and Applied Fracture Mechanics*, 2019, **99**, 44-50.
33. P. K. Szewczyk, A. Gradys, S. K. Kim, L. Persano, M. Marzec, A. Kryshtal, T. Busolo, A. Toncelli, D. Pisignano, A. Bernasik, S. Kar-Narayan, P. Sajkiewicz and U. Stachewicz, *ACS Appl. Mater. Interfaces*, 2020, **12**, 13575-13583.
34. I. P. Seshadri and B. Bhushan, *J. Colloid Interf. Sci.*, 2008, **325**, 580-587.
35. T. Bahners, U. Schlosser, R. Gutmann and E. Schollmeyer, *Solar Energy Materials and Solar Cells*, 2008, **92**, 1661-1667.
36. T. J. Dawson, K. N. Webster and S. K. Maloney, *Journal of Comparative Physiology B-Biochemical Systemic and Environmental Physiology*, 2014, **184**, 273-284.
37. H. Jia, J. Zhu, Z. Li, X. Cheng and J. Guo, *Solar Energy Materials and Solar Cells*, 2017, **159**, 345-351.
38. H. E. M. Liwanag, A. Berta, D. P. Costa, S. M. Budge and T. M. Williams, *Biological Journal of the Linnean Society*, 2012, **107**, 774-787.
39. A. R. M. Müllner, R. Pahl, D. Brandhuber and H. Peterlik, *Molecules (Basel, Switzerland)*, 2020, **25**, 2143.
40. S. Metwally, S. M. Comesana, M. Zarzyka, P. K. Szewczyk, J. E. Karbowniczek and U. Stachewicz, *Acta Biomater*, 2019, **91**, 270-283.
41. H. Jia, J. Guo and J. Zhu, *Journal of Bionic Engineering*, 2017, **14**, 616-621.
42. P. L. Pap, G. Osvath, T. Daubner, A. Nord and O. Vincze, *Evolution*, 2020, **74**, 2365-2376.
43. M. J. Greenwold, W. Bao, E. D. Jarvis, H. Hu, C. Li, M. T. P. Gilbert, G. Zhang and R. H. Sawyer, *Bmc Evolutionary Biology*, 2014, **14**.
44. M. Eder, S. Amini and P. Fratzl, *Science*, 2018, **362**, 543.
45. S. Metwally and U. Stachewicz, *Micron*, 2020, **137**, 102913.
46. D. D. Arola and J. A. Rouland, *J. Biomed. Mater. Res. A*, 2003, **67A**, 78-86.
47. S. Inoue, P. N. R. Pereira, C. Kawamoto, M. Nakajima, K. Koshiro, J. Tagami, R. M. Carvalho, D. H. Pashley and H. Sano, *Dental Materials Journal*, 2003, **22**, 39-47.
48. N. S. Ha and G. Lu, *Composites Part B: Engineering*, 2020, **181**, 107496.
49. D. Leguillon and R. Piat, *Eng. Fract. Mech.*, 2008, **75**, 1840-1853.
50. H. Peterlik, P. Roschger, K. Klaushofer and P. Fratzl, *Nat. Mater.*, 2006, **5**, 52-55.
51. C. T. Koh and M. L. Oyen, *APL Materials*, 2015, **3**.
52. M. Mirkhalaf, A. K. Dastjerdi and F. Barthelat, *Nature Communications*, 2014, **5**.
53. S. Jiang, J. Y. Cheong, J. S. Nam, I.-D. Kim, S. Agarwal and A. Greiner, *ACS Appl. Mater. Interfaces*, 2020, **12**, 19006-19014.